Hybrid identification with time-series data and frequency response data for accurate estimation of linear characteristics

1st Ryohei Kitayoshi
Tsukuba Research Laboratory Corporate Technology Division
YASKAWA Electric Corporation
9-10 Tokodai 5 Chome, Tsukuba, Ibaraki, Japan
Ryohei.Kitayoshi@yaskawa.co.jp

2nd Hiroshi Fujimoto
Graduate School of Frontier Sciences
The University of Tokyo
5-1-5, Kashiwanoha, Kashiwa, Chiba, 277-8561, Japan
fujimoto@k.u-tokyo.ac.jp

***Abstract*—The purpose of this paper is to estimate the linear characteristics accurately by separating the nonlinear characteristics from the time-series data that measures the frequency response characteristics of the plant. In general, it has not been easy to separate linear and nonlinear characteristics because measurement data includes both of the characteristics. However, it is possible to separate by assuming a model of nonlinear characteristics, searching for parameters of the nonlinear model, and estimating transfer function from the Frequency Response Data (FRD) without the effect of the nonlinearity. We call this method hybrid identification of time-series data and frequency data since FRD is used to estimate the linear transfer function, and time-series data is used to estimate the parameters of nonlinear characteristics. Moreover, Bayesian optimization is used as an efficient search method of the parameters of the nonlinear model. The effectiveness of the proposed identification method is verified by ball screw and rolling friction.**

***Index Terms*—hybrid identification, rolling friction, Bayesian optimization, linear characteristics, ball screw**

I. Introduction

In recent years, industrial machines have become low-rigidity for cost reduction, while operations speed and accuracy have been requested to improve for higher throughputs. As a result, the servo controller adjustment has become more complicated and, it has been more important to know and utilize the machine's characteristics in detail.

Therefore, researches on data-driven controller design [1] have been conducted to adjust and design the controller automatically. In particular, the automatic adjustment method based on Frequency Response Data (FRD) [2], [3] is an excellent and easy-to-use method because the controller's stability and the range of design parameters can be used as constraints for controller design.

When utilizing the data-driven method, the accurate linear characteristics of the machine are needed. However, it is not easy to measure only the linear characteristics due to the machine's nonlinear characteristics. For the measurement of nonlinear characteristics, different experiments with special conditions must be done. These extra experiments are time-consuming and are not desirable for machine users.

978-1-7281-4442-9/21/$31.00 ©2021 IEEE

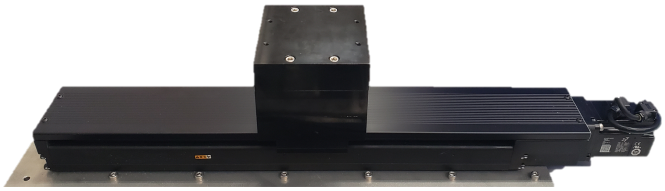

Fig. 1. Overview of the ball screw drive system

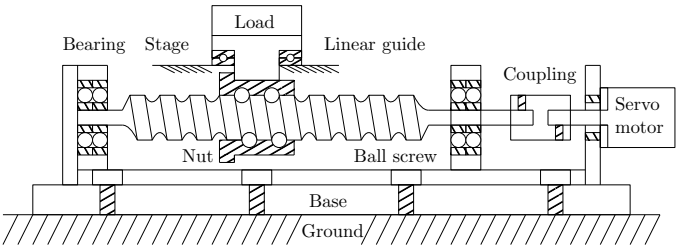

Fig. 2. Schematic drawing of the ball screw drive system

Therefore, we proposed a novel method for estimating linear characteristics accurately by separating nonlinear characteristics from one time-series data when obtaining FRD. The proposed method assumes that only the machine's nonlinearity model is known and makes it possible to separate the linearity and the nonlinearity by searching for the nonlinear model's parameters and estimating transfer function from the FRD without the effect of the nonlinearity. The effectiveness of the proposed method is verified with a ball screw.

The nonlinearity assumed in this paper is rolling friction, which is a common characteristic in ball screws. Rolling friction is caused by the nonlinear elasticity of rolling elements and coulomb friction [4]. It has been the subject of research for a long time as a factor that deteriorates precision positioning control [5], [6]. Various models such as the LuGre model [7] and the Koizumi model [8] have been proposed to express the nonlinear characteristics. In particular, in recent years, a method for accurately expressing friction characteristics using a rheology model [9], [10] has been proposed, and its

TABLE I
SPECIFICATIONS OF THE BALL SCREW DRIVE SYSTEM

Item	Value	Units
Weight of the load	6.0	kg
Inertia of the servomotor	1.39×10^{-5}	kg·m^2
Total inertia of the system	15.29×10^{-5}	kg·m^2
Rated torque	0.637	N·m

application to FF controllers [11], [12] has also been reported. The study on simultaneous identification of the rolling friction and the linear characteristics parameters [13] was conducted by driving the ball screw with multiple low-frequency position reference. The study on suppressing rolling friction with RPTC (Repetitive Perfect Tracking Control) was conducted [14]. From the above, we use the rheology model as a nonlinear model of the rolling friction.

The constitution of this paper is as follows. In section. II, mechanism, and frequency characteristics of ball screw and rolling friction characteristics are described. In section. III, the proposed identification method of frequency characteristics and nonlinear friction characteristics is explained. In section. IV, for validation of the proposed method, a comparison result with measurement and analysis of the proposed method is illustrated. At last, in section. V, a summary of this paper, and prospects of this research are shown.

II. MECHANISM AND DYNAMIC CHARACTERISTICS OF BALL SCREW

A. Mechanism of ball screw drive system

A ball screw drive system in Fig.1 consists of a servomotor, a servo driver, a ball screw, and a load. The servomotor and servo driver are products of YASKAWA Electric corporation products (model: SGM7A-02A7A and SGD7S-1R6A) with a 24-bit encoder. The ball screw has a 20 mm lead (20 mm/rotation). The load is on the table, and its weight is 6 kg. Other specifications of the ball screw drive system are shown in Table.I.

B. Frequency characteristics and rolling friction

Generally, the ball screw drive system's rigidity is very high, and it is very useful for precise positioning. However, there are many fastening components and support components in Fig. 2: bearing, coupling, nut, et cetera. These components cause the ball screw to have multiple vibration modes. The vibration modes make it difficult to adjust controller parameters and deteriorate positioning accuracy. Therefore, we need to know the frequency characteristics precisely.

However, the nonlinear friction often prevents from obtaining the accurate frequency characteristics. Notably, it is known that in the case of the ball screw drive system, rolling friction reduces gain at low frequencies [5], [9]. The rolling friction characteristics are shown in Fig. 3. The region1 is the pre-rolling region where nonlinear elastic characteristics dominate. The region2 is the rolling region where coulomb friction is dominant. The frictional characteristics can be expressed as

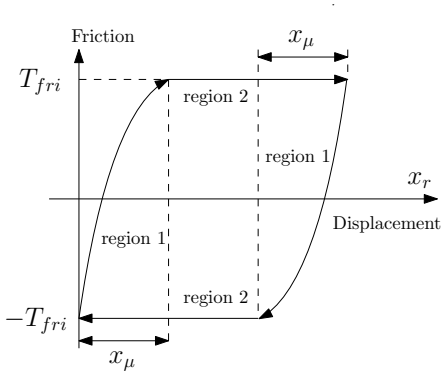

Fig. 3. Rolling friction characteristics

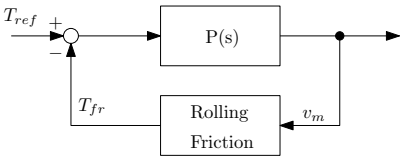

Fig. 4. Nonlinear system including rolling friction and the linear characteristics of the ball screw: P(s)

in (1)∼(2) with the rheology model [9], [15]. The rheology model is the multi-structure.

$$x_i = \begin{cases} x + x_{ri} & (|x_i < X_{mi}|) \\ sgn(v_m) \cdot X_{mi} & (|x_i > X_{mi}|) \end{cases} \tag{1}$$

$$T_{fr} = K_i x_i + D_i \frac{dx_i}{dt} \tag{2}$$

The magnitude of rolling friction depends on the displacement from the time of speed reversal. Since rolling friction T_{fr} is added to the torque reference T_{ref} as a disturbance, the nonlinear system is expressed in (3), including the linear characteristics of the ball screw. From (3), the actual input torque to the ball screw is $T_{ref} - T_{fr}$ in Fig.4 [16], and it is essential to estimate T_{fr} to identify the linear characteristics of the ball screw accurately.

$$V_m(s) = P(s) \cdot (T_{ref} - T_{fr}) \tag{3}$$

As shown in Fig.4, linearity and nonlinearity are represented by different blocks. This modeling is called the block-oriented model [17], [18], [19], and is the basic idea for separating linearity and nonlinearity from the time-series data.

III. HYBRID IDENTIFICATION WITH TIME-SERIES DATA AND FREQUENCY RESPONSE DATA

In this section, the proposed hybrid identification with time-series data and frequency response data is explained. The proposed method consists of six steps shown in Fig.5.

A. Flow of the proposed identification method

Step.1: Measurement of time-series input/output data
The excitation torque signal $\tau_{ref}(t)$ is periodically inputted to the plant ten times to acquire the output velocity data $v_m(t)$.

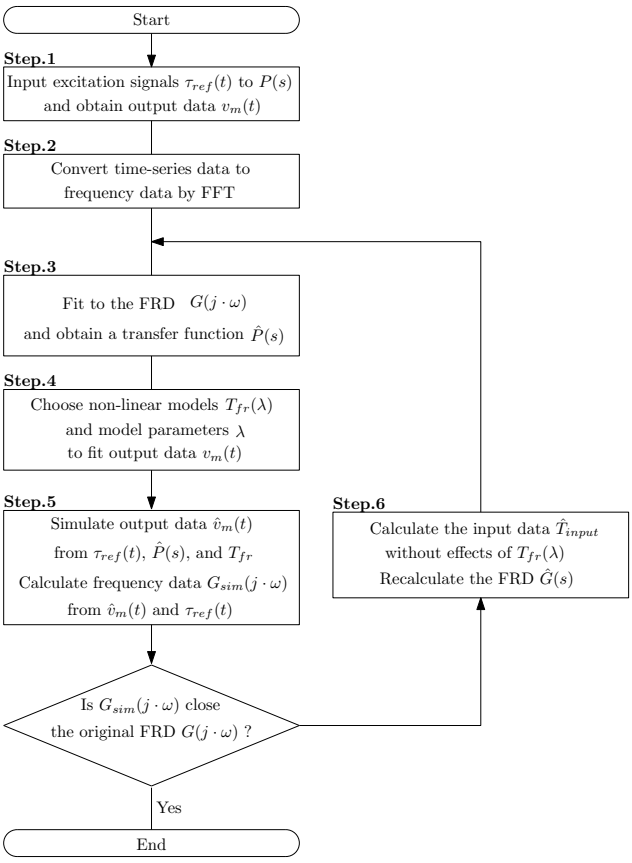

Fig. 5. Flowchart of the proposed hybrid system identification

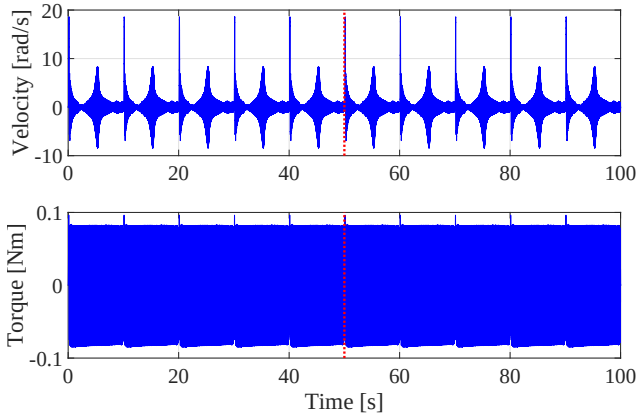

Fig. 6. Measurement of torque reference $\tau_{ref}(t)$ and motor velocity $v_m(t)$

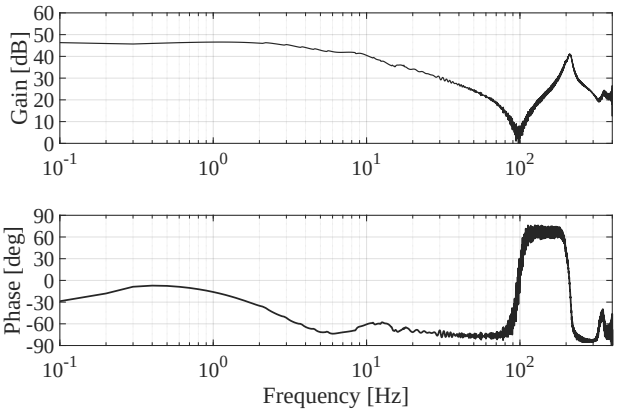

Fig. 7. FRD of the ball screw (input: $\tau_{ref}(t)$, output: $v_m(t)$)

The input/output data is shown in Fig.6. The excitation signal is a chirp signal in (4) and (5). The chirp signal is easy to determine the frequency range which the user wants to excite. The frequency range $\omega_i(t)$ changes from 0.1 Hz to 400 Hz, and the measurement time t_{meas} and the sampling period are 10 s, 125 μs, respectively. The initial frequency ω_0 is $0.1\cdot 2\pi$ rad/s, and the final frequency ω_1 is $400\cdot 2\pi$ rad/s. The initial phase of the signal ϕ_0 is 0 deg. The signal amplitude A is 0.0764 N·m (12% of the rated motor torque), which value is determined so that the motor rotation angle according to ten input signals is less than one rotation. This is because large movement may cause change of resonance frequency.

$$\tau_{ref}(t) = A\cdot\sin\Big(\omega_i(t)\cdot t+\phi_0\Big) \tag{4}$$

$$\omega_i(t) = \omega_0 + (\omega_1-\omega_0)\cdot\frac{t}{t_{meas}} \quad (0\le t\le t_{meas}) \tag{5}$$

Step.2: Obtaining Frequency Response Data (FRD)

Fourier transform is applied to the time-series input/output data $\tau_{ref}(t)$, $v_m(t)$ to acquire the FRD of the plant $G(j\cdot\omega)$. The obtained FRD is shown in Fig.7. The frequency resolution is 0.1 Hz. The FRD is calculated from the time-series data from 50 s to 100 s. The red dashed line in Fig.6 illustrates 50 s. The reason for not using the first half of the data is that the output data at the beginning of the excitation may not converge to steady states.

Step.3: Estimating transfer function

The linear transfer function $\hat{P}(s)$ is estimated by fitting for the FRD $G(j\cdot\omega)$. The fitting method is based on least-squares [20]. The numerator and denominator degree was set as 4 and 5 ($n=4, m=5$) because there is at least one vibration mode from the FRD.

$$\hat{P}(s) = \frac{b_n s^n + b_{n-1}s^{n-1}+\cdots b_0}{s^m + a_{m-1}s^{m-1}+\cdots+a_0} \tag{6}$$

Step.4: Searching the nonlinear model's parameters based on Bayesian optimization

The approximate model of rolling friction $T_{fr}(\lambda,t)$ is prepared in (7)∼ (9) based on the rheology model in Fig.8. The model parameters λ are searched from a search range Λ in Table.II to match the time-series output data $v_m(t)$ and the simulated output data $\hat{v}_m(t)$ in (13). The search method of the nonlinear model parameters is Bayesian optimization explained in III-C.

$$\hat{T}_{fr} = \begin{cases} T_{rev}+\mathrm{sgn}(v_m(t))\cdot K_2\cdot x_r & (0\leqq|x_r|<X_2)\\ T_{rev}+\mathrm{sgn}(v_m(t))\cdot\{T_2+K_1(x_r-X_2)\} & (X_2\leqq|x_r|\leqq X_1)\\ \mathrm{sgn}(v_m(t))\cdot T_1 & (X_1<|x_r|)\end{cases} \tag{7}$$

$$K_1 = (T_1-T_2)/(X_1-X_2) \tag{8}$$

$$K_2 = (T_1+T_2)/X_2 \tag{9}$$

TABLE II
SEARCH RANGE Λ OF ROLLING FRICTION PARAMETERS

Symbol	Min	Max	Unit
X_1	50	150	μm
X_2	10	49	μm
T_1	2.55×10^{-2} (4.0)	6.37×10^{-2} (10.0)	N·m(%)
T_2	6.37×10^{-3} (1.0)	2.48×10^{-2} (3.9)	N·m(%)

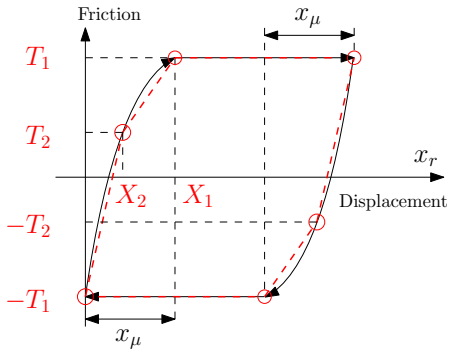

Fig. 8. Approximate model of the rolling friction

In the above, T_{rev} is the torque value when velocity reversal. K_1 and K_2 are elastic coefficients in the divided region.

$$\hat{T}_{input} = T_{ref} - \hat{T}_{fr} \tag{10}$$

$$\hat{v}_m = \hat{P}(s) \cdot \hat{T}_{input} \tag{11}$$

$$v_{err} = \sum_{i=1}^{\ell} ||v_m(i) - \hat{v}_m(i))||^2 \tag{12}$$

$$\lambda^* = \arg\min_{\lambda\in\Lambda} v_{err} \tag{13}$$

$$\lambda = [X_1, X_2, T_1, T_2] \tag{14}$$

Step.5: Simulating output data and FRD based on the estimated transfer function and nonlinear model
To verify the estimation results, output data $\hat{v}_m(t)$ is generated from (11) in Step.3. Simulated FRD: $G_{sim}(j\cdot\omega)$ is produced from $\tau_{ref}(t)$ and $\hat{v}_m(t)$. If $G_{sim}(j\cdot\omega)$ is close enough to $G(j\cdot\omega)$, the identification process is terminated. If it cannot be reproduced, perform Step.6.
Step.6: Calculating input/output data without effect of the nonlinear model and recalculating the frequency data
After removing the nonlinear model's influence from the time-series input/output data, the FRD is regenerated from (15) and (16). The linear transfer function $\hat{P}(s)$ is estimated from the regenerated FRD $\hat{G}(j\cdot\omega)$ again in Step.3.

$$\hat{T}_{input} = T_{ref} - \hat{T}_{fr} \tag{15}$$

$$\hat{G}(j\cdot\omega) = \frac{V_m}{\hat{T}_{input}} \tag{16}$$

B. Convergence of the estimated results

To guarantee the convergence of the estimated results, the velocity error at k time $v_{err}[k]$ is saved. Among the error up to the kth time, the minimum velocity error is the best value written asJ_{best}. If the $k+1$ th velocity error $v_{err}[k+1]$ is less than J_{best}, $G(j\cdot\omega)$ is replaced by $\hat{G}(j\cdot\omega)$ in Step.3.

$$J_{best} = \min\{v_{err}[N], N = 1, 2, \cdots, k\} \tag{17}$$

C. Bayesian optimization: a search method for parameters of nonlinear model

Bayesian optimization is one of the optimization methods for the black-box optimization problem whose objective function is unknown. The representative black-box optimization problem is the hyperparameter search of Neural Networks or Support Vector Machine [21]. Commonly, the random search and the grid search have been used, but Bayesian optimization has been focused as a more efficient search method based on the Gaussian process. In recent years, not only in the field of machine learning but also in the field of control engineering, the application of Bayesian optimization was reported for parameter tuning of the controller in the nonlinear system [22].

Bayesian optimization is expressed in (18) $\sim$ (21). A vector of hyperparameters is denoted by $\lambda \in \Lambda$. The objective function is denoted by $L(\lambda)$. The expected improvement in (20) and (21) is used as the acquisition function. The improvement of at the combination of the parameters λ is expressed in (19).

$$\lambda^* = \arg\min_{\lambda\in\Lambda} L(\lambda) \tag{18}$$

$$I(\lambda) = \max(f_{min} - y, 0) \tag{19}$$

$$E[I(\lambda)] = E[\max(f_{min} - y, 0)] \tag{20}$$

$$E[I(\lambda)] = (f_{min} - \mu(\lambda))\Phi\left(\frac{f_{min} - \mu(\lambda)}{\sigma}\right) + \sigma\phi\left(\frac{f_{min} - \mu(\lambda)}{\sigma}\right) \tag{21}$$

In the above, ϕ and Φ are the standard normal density and distribution function. The symbol μ, σ and f_{min} express the current best value respectively.

IV. EXPERIMENT FOR VALIDIATION

A. Measurement condition of rolling friction

We obtained the measurement of rolling friction. Position and torque reference was measured when the motor was driven with triangle four position reference: 50 µm, 100 µm, 200 µm, and 400 µm. The position reference is in a periodic triangle shape with a frequency of 0.33 Hz. The measurement in the case of 200 µm is shown in Fig. 9.

The friction torque T_{fr} was calculated from the position x_m and torque reference T_{ref} in (22). In this equation, the torque generated by acceleration and deceleration is removed from the torque reference, and the remaining value is calculated as friction torque. The low pass filter is used for withdrawing the noise, and its cutoff frequency is set as $10 \times 2\pi$ rad/s. The cutoff frequency is higher enough than the frequency of position reference: 0.33 Hz.

$$T_{fr} = \left(T_{ref} - J_{all} \cdot x_m \cdot s^2\right) \cdot \frac{\omega_{lpf}}{s + \omega_{lpf}} \tag{22}$$

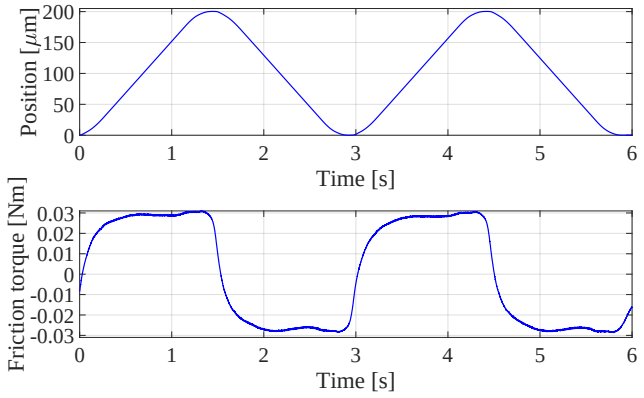

Fig. 9. Measument of position and friction torque in the case of 400 µm

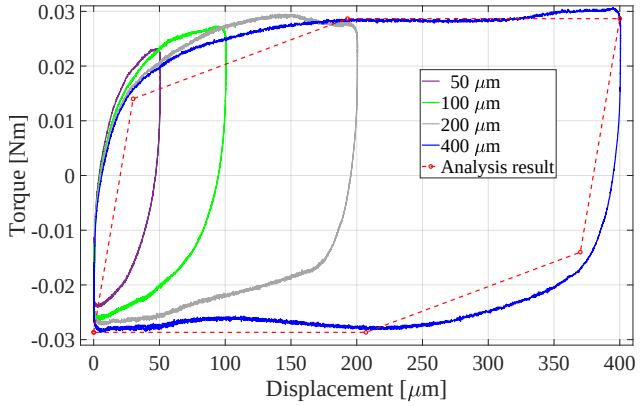

Fig. 10. Measurement of rolling friction (blue: displacement 400 µm, gray: displacement 200 µm, and green: displacement 100 µm, purple: displacement 50 µm, and red dashed: the analysis result of nonlinear model)

B. Measurement result of rolling friction

The measurement result of rolling friction is shown in Fig.10. The maximum friction value is 2.74×10^{-2} N·m (4.3 % of the rated motor torque). The pre-rolling region is less than 50 µm. The rolling region seems to be more than 200 µm.

C. Comparison for analysis result and measurement

The analysis results of linear characteristics and nonlinear friction are shown in Table.III, IV, and (23).

1) Rolling friction: The maximum value of the rolling friction is 2.87×10^{-2} N·m (4.5% of the motor rated torque), that is close to the measurement result: 2.74×10^{-2} N·m (4.3% of the motor rated torque). The region1 is very narrow and has a displacement of 10 µm, while region2 is in the range of about 90 µm.

2) Linear characteristics of the ball screw: We obtained the transfer function $\hat{P}(s)$ in (23) and Table.IV.The estimated transfer function $\hat{P}(s)$ has an oscillation mode(anti-resonance frequency: 97.0 Hz and resonance frequency: 208.1 Hz), and matches the frequency response data well from Fig. 11. While at the low frequency band the gain of the trasfer function $\hat{P}(s)$ is higher than the experiment data (FRD), the result of removing the influence of rolling friction can be confirmed.

TABLE III
ANALYSIS RESULTS OF ROLLING FRICTION

Symbol	Analysis value	Unit
X_1	193	µm
X_2	30	µm
T_1	2.87×10^{-2} (4.5)	N·m (%)
T_2	1.40×10^{-2} (2.2)	N·m (%)

TABLE IV
ANALYSIS RESULTS OF FREQUENCY CHARACTERISTICS

Symbol	Value	Symbol	Value	Unit
ω_{r1}	$208.1 \times 2\pi$	ω_{r2}	$340.5 \times 2\pi$	rad/s
ζ_{r1}	4.56×10^{-2}	ζ_{r2}	0.623	-
ω_{a1}	$97.0 \times 2\pi$	ω_{a2}	$291.3 \times 2\pi$	rad/s
ζ_{a1}	7.17×10^{-2}	ζ_{a2}	0.329	-
K	3.38×10^{4}	-	-	-

$$\hat{P}(s) = \frac{K}{s(s+8.725)} \cdot \prod_{i=1}^{2} \frac{s^2 + 2\zeta_{ai}\omega_{ai}s + \omega_{ai}^2}{s^2 + 2\zeta_{ri}\omega_{ri}s + \omega_{ri}^2} \quad (23)$$

3) Frequency response data of the ball screw: The frequency response data was reproduced in Fig.11 to confirm that the combination of the estimated transfer function and the analyzed nonlinear model is appropriate. It was confirmed that the reproduced FRD (a blue line in Fig.11) accurately matched the experimental data (a black line in Fig.11). In particular, at the low frequency band (0.1 $\sim$ 2.0 Hz), the error of both data is less than 1 dB for gain and 5 deg for phase.

4) Convergence of the velocity error: To confirm the convergence of the estimated results, the velocity error v_{err} is shown in Fig.13. The horizontal axis shows the number of times the estimation flow was executed. The blue line shows v_{err} at each time, and the green line shows the best value J_{best} up to the current time. From Fig.13, it can be confirmed that the best value of the estimated results is converged.

V. CONCLUSION

This paper proposed the hybrid identification method with time-series data and frequency response data for obtaining the precise linear characteristics of the plant and nonlinear friction characteristics. For validation for the proposed method, we conducted the measurement of rolling friction and frequency response data of the ball screw, and the proposed method's analysis results were compared with measurement. As a result, low-frequency characteristics are improved, and rolling friction characteristics match the measurement and the analysis results. Moreover, Bayesian optimization was used for an efficient search method of the nonlinear model's parameters, and we obtained the appropriate value which matched the measurement.

We have planned to automatically adjust the position controller with obtained linear characteristics and the friction model and parameters. We aim to realize data-driven high precision control.

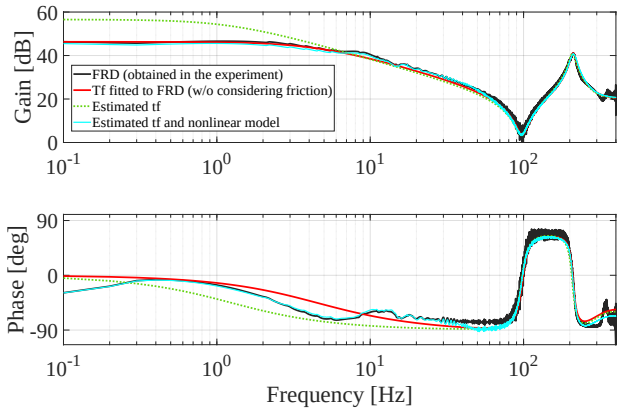

Fig. 11. Comparison for frequency response data (black: experiment data, red: transfer function fitted to FRD, green dashed: the estimated transfer function, and blue: the estimated transfer function and nonlinear model)

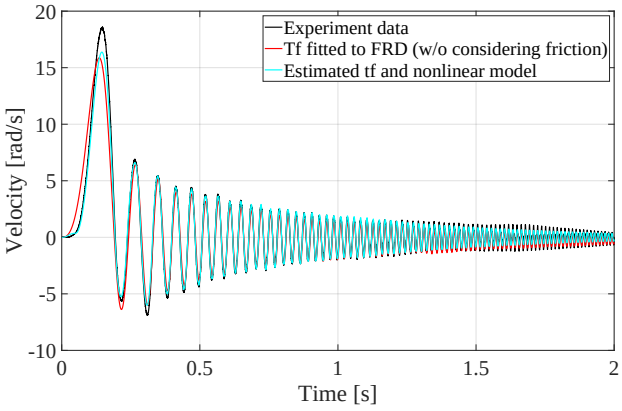

Fig. 12. Comparison for time-series data of velocity (black: experiment data, red: transfer function fitted to FRD, and blue: the estimated transfer function and nonlinear model)

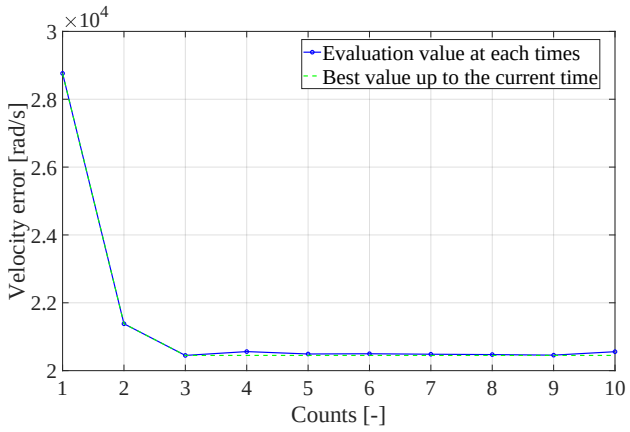

Fig. 13. Convergence of the best value of the velocity error (blue: velocity error at each estimation time and green: the best value J_{best} up to the current time)

REFERENCES

[1] J. Swevers, L. Jacobs, T. Singh, D. Turk, M. Verbandt, and G. Pipeleers, "LCToolbox: Facilitating Optimal Linear Feedback Controller Design," *IEEJ Journal of Industry Applications*, vol. 9, no. 2, pp. 109–116, mar 2020.

[2] P. Apkarian and D. Noll, "Nonsmooth H ∞ Synthesis," *IEEE Transactions on Automatic Control*, vol. 51, no. 1, pp. 71–86, jan 2006.

[3] ——, "Structured H ∞ -control of infinite-dimensional systems," *International Journal of Robust and Nonlinear Control*, vol. 28, no. 9, pp. 3212–3238, jun 2018.

[4] F. Al-Bender and J. Swevers, "Characterization of friction force dynamics," *IEEE Control Systems*, vol. 28, no. 6, pp. 64–81, dec 2008.

[5] S. Futami, A. Furutani, and S. Yoshida, "Nanometer positioning and its micro-dynamics," *Nanotechnology*, vol. 1, no. 1, pp. 31–37, jul 1990.

[6] J. Otsuka and T. Masuda, "The influence of nonlinear spring behavior of rolling elements on ultraprecision positioning control systems," *Nanotechnology*, vol. 9, no. 2, pp. 85–92, jun 1998.

[7] C. Canudas de Wit, H. Olsson, K. Astrom, and P. Lischinsky, "A new model for control of systems with friction," *IEEE Transactions on Automatic Control*, vol. 40, no. 3, pp. 419–425, mar 1995.

[8] T. Koizumi and H. Shibazaki, "A study of the relationships governing starting rolling friction," *Wear*, vol. 93, no. 3, pp. 281–290, feb 1984.

[9] Y. Maeda and M. Iwasaki, "Rolling Friction Model-Based Analyses and Compensation for Slow Settling Response in Precise Positioning," *IEEE Transactions on Industrial Electronics*, vol. 60, no. 12, pp. 5841–5853, dec 2013.

[10] Y. Maeda, K. Harata, and M. Iwasaki, "A Friction Model-Based Frequency Response Analysis for Frictional Servo Systems," *IEEE Transactions on Industrial Informatics*, vol. 14, no. 11, pp. 5146–5155, nov 2018.

[11] Y. Maeda and M. Iwasaki, "Feedforward Friction Compensation Using the Rolling Friction Model for Micrometer-stroke Point-to-point Positioning Motion," *IEEJ Journal of Industry Applications*, vol. 7, no. 2, pp. 141–149, 2018.

[12] T. Hayashi, H. Fujimoto, Y. Isaoka, and Y. Terada, "Projection-based Iterative Learning Control for Ball-screw-driven Stage with Consideration of Rolling Friction Compensation," *IEEJ Journal of Industry Applications*, vol. 9, no. 2, pp. 132–139, mar 2020.

[13] T. Takemura and H. Fujimoto, "Simultaneous identification of linear parameters and nonlinear rolling friction for ball screw driven stage," in *IECON 2011 - 37th Annual Conference of the IEEE Industrial Electronics Society*. IEEE, nov 2011, pp. 3424–3429.

[14] H. Fujimoto and T. Takemura, "High-Precision Control of Ball-Screw-Driven Stage Based on Repetitive Control Using n-Times Learning Filter," *IEEE Transactions on Industrial Electronics*, vol. 61, no. 7, pp. 3694–3703, jul 2014.

[15] G. Ferretti, G. Magnani, and P. Rocco, "Single and Multistate Integral Friction Models," *IEEE Transactions on Automatic Control*, vol. 49, no. 12, pp. 2292–2297, dec 2004.

[16] Yung-Yaw Chen, Pai-yi Huang, and Jia-Yush Yen, "Frequency-domain identification algorithms for servo systems with friction," *IEEE Transactions on Control Systems Technology*, vol. 10, no. 5, pp. 654–665, sep 2002.

[17] J. Schoukens and L. Ljung, "Nonlinear System Identification: A User-Oriented Road Map," *IEEE Control Systems Magazine*, vol. 39, no. 6, December, pp. 28–99, 2019.

[18] A. F. Esfahani, J. Schoukens, and L. Vanbeylen, "Using the Best Linear Approximation with Varying Excitation Signals for Nonlinear System Characterization," *IEEE Transactions on Instrumentation and Measurement*, vol. 65, no. 5, pp. 1271–1280, 2016.

[19] L. Vanbeylen, "Nonlinear LFR Block-Oriented Model: Potential Benefits and Improved, User-Friendly Identification Method," *IEEE Transactions on Instrumentation and Measurement*, vol. 62, no. 12, pp. 3374–3383, dec 2013.

[20] Z. Drmač, S. Gugercin, and C. Beattie, "Quadrature-Based Vector Fitting for Discretized H2 Approximation," *SIAM Journal on Scientific Computing*, vol. 37, no. 2, pp. A625–A652, jan 2015.

[21] K. Grąbczewski, *Automated Machine Learning*, ser. The Springer Series on Challenges in Machine Learning, F. Hutter, L. Kotthoff, and J. Vanschoren, Eds. Cham: Springer International Publishing, 2019, vol. 498.

[22] M. Neumann-Brosig, A. Marco, D. Schwarzmann, and S. Trimpe, "Data-Efficient Autotuning With Bayesian Optimization: An Industrial Control Study," *IEEE Transactions on Control Systems Technology*, vol. 28, no. 3, pp. 730–740, may 2020.